



HAL
open science

Failure mechanisms in granular media: a discrete element analysis

François Nicot, Nejib Hadda, Franck Bourrier, Luc Sibille, Félix Darve

► **To cite this version:**

François Nicot, Nejib Hadda, Franck Bourrier, Luc Sibille, Félix Darve. Failure mechanisms in granular media: a discrete element analysis. *Granular Matter*, 2011, 13 (3), pp.255-260. 10.1007/s10035-010-0242-3 . hal-02595710

HAL Id: hal-02595710

<https://hal.inrae.fr/hal-02595710v1>

Submitted on 18 Sep 2024

HAL is a multi-disciplinary open access archive for the deposit and dissemination of scientific research documents, whether they are published or not. The documents may come from teaching and research institutions in France or abroad, or from public or private research centers.

L'archive ouverte pluridisciplinaire **HAL**, est destinée au dépôt et à la diffusion de documents scientifiques de niveau recherche, publiés ou non, émanant des établissements d'enseignement et de recherche français ou étrangers, des laboratoires publics ou privés.



Distributed under a Creative Commons Attribution - NonCommercial 4.0 International License

Failure mechanisms in granular media: a discrete element analysis

François Nicot, Nejb Hadda, Franck Bourrier, Luc Sibille, Félix Darve

Abstract This paper attempts to numerically validate the concept of diffuse failure using a discrete element method. First, the theoretical background is reviewed, and it is shown how the kinetic energy of a system, initially at rest after a loading history, is likely to abruptly increase under the effect of disturbances. The vanishing of the second-order work thus constitutes a basic ingredient, related to both the pioneering work of Hill (J Mech Phys Solids (6):236–249, 1958) and the notion of bifurcation applied to geomechanics (Vardoulakis and Sulem in Bifurcation analysis in geomechanics, Chapman & Hall Publisher, London, 1995). Discrete numerical simulations were performed on homogeneous three-dimensional specimens, and the three basic conditions that must be satisfied in order to observe a failure mechanism are numerically checked. Finally, this work illustrates the phenomena that are likely to affect in situ slopes, for instance, when the loading (due to weather conditions or human activities) meets the three basic conditions for a failure mechanism to develop.

Keywords Bifurcation · Sustainability · Second-order work · Loading parameters · Discrete element method · Diffuse failure · Collapse

F. Nicot (✉) · N. Hadda · F. Bourrier
CEMAGREF, Grenoble, France
e-mail: francois.nicot@cemagref.fr

L. Sibille
Institut de Recherche en Génie Civil et Mécanique, Université de
Nantes, ECN-CNRS, Nantes, France

F. Darve
UJF-INPG-CNRS, Laboratoire Sols Solides Structures Risques,
Grenoble, France

1 Introduction

One of the first contributions of Vardoulakis to building rational geomechanics was to consider shear band formation as a bifurcation problem [18,20]. Indeed bifurcation viewed as a particular case of catastrophe (in the sense of the catastrophe theory, [17]) corresponds to physical states where the shape/state of a system suddenly changes under continuous variations of the loading parameters. According to experimental evidence [19] shear bands indeed appear abruptly during a continuous application of loading. More generally, failure in geomechanics can be analysed as a bifurcation phenomenon with loss of uniqueness and loss of stability (it should be noted that bifurcation does not necessarily imply either loss of uniqueness or loss of stability) and this seems to be true for any kind of failure mode by divergence [5].

To analyse failure in non-associate materials, one criterion plays a particular role: this is the so-called second-order work criterion [1,20,5] because—if we except flutter instabilities—this is the first to be met along a given loading path and it contains all the other classical criteria such as plastic limit conditions and strain localisation criteria [2,3,11]. However, this second-order work criterion has to be used very carefully to avoid presumable counter-examples. Clarifying the conditions for utilising this criterion properly is the main objective of this paper.

So, more precisely, three necessary and sufficient conditions have to be fulfilled for true material failure:

- The stress state has to be inside the bifurcation domain;
- The loading direction has to be inside an instability cone;
- Proper loading variables have to be chosen.

If one of these three conditions is not fulfilled, failure will not occur even if the second-order work takes strictly

negative values. The second-order work criterion is no more than a necessary condition for failure. On the other hand and by excepting flutter instabilities, a strictly positive second-order work in all loading directions (i.e. for all disturbances) is a sufficient condition of stability [7], excluding any kind of material failure. The purpose of this paper is therefore to investigate these three necessary and sufficient conditions for failure.

This requires a numerical method able to describe a failure mechanism in detail. Today it seems that only molecular dynamics methods give reliable and robust results for the development of a failure mechanism, including pre- and post-failure regimes. Thus a discrete element method [8] has been used.

In the first part of this paper, the theoretical background of the second-order work criterion is reviewed, then discrete element results are presented and discussed to check the validity of these three necessary and sufficient conditions for material failure.

2 An approach to failure in soil mechanics

2.1 The theoretical framework

A series of studies have shown that the occurrence of failure could be described properly from the vanishing of the second-order work [6, 12, 13, 11]. The purpose of this section is to briefly review the theoretical background, investigating how the kinetic energy of a system initially in equilibrium can rise under the application of a certain disturbance class. For this purpose, a system made up of a volume V_o of a given material, initially in a configuration C_o (initial configuration) is considered. \underline{b}_o denotes the initial body force density field. After a loading history, the system is in a strained configuration C and occupies a volume V , with a body force density field \underline{b} , in equilibrium under a prescribed external loading. An external stress distribution \underline{f} acts on the current boundary (Γ) of the material.

The instantaneous evolution of the system, in the equilibrium configuration C at time t , is governed by the following kinetic energy equation that includes dynamical effects:

$$\delta E_c(t) = \int_{\Gamma_o} F_i \delta u_i dS_o + \int_{V_o} b_{o,i} \delta u_i dV_o - \int_{V_o} \Pi_{ij} \frac{\partial(\delta u_i)}{\partial X_j} dV_o \quad (1)$$

where δE_c represents the system's current change in kinetic energy, and $\delta \underline{u}$ is the incremental displacement field. As will be seen later, both translational and rotational velocities of particles have to be accounted for to compute the whole kinetic energy of a granular assembly [21]. $\underline{\Pi}$ denotes the

Piola-Kirchoff stress tensor of the first type, and Γ_o is the V_o boundary. $\underline{\Pi}$ (respectively \underline{F}) is the transformed quantity of the Cauchy stress tensor $\underline{\sigma}$ (resp. \underline{f}) through the bijection ϑ mapping the material points from the reference configuration to the current configuration: $\underline{x} = \vartheta(\underline{X})$. The time differentiation of Eq. (1) can be performed in a straightforward manner, without referring to a Reynolds transform. Taking into account Green's formula, differentiating Eq. (1) gives [12]:

$$\delta^2 E_c(t) = \int_{\Gamma_o} \delta F_i \delta u_i dS_o + \int_{V_o} \delta b_{o,i} \delta u_i dV_o - \int_{V_o} \delta \Pi_{ij} \frac{\partial(\delta u_i)}{\partial X_j} dV_o \quad (2)$$

Following Hill's definition [7], $W_2 = \int_{V_o} \delta \Pi_{ij} \frac{\partial(\delta u_i)}{\partial X_j} dV_o$ denotes the second-order work of the system. Ignoring incremental geometrical changes, the second-order work can also be expressed as:

$$W_2 = \int_{V_o} \delta \sigma_{ij} \delta \varepsilon_{ij} dV_o \quad (3)$$

Thus, Eq. (3) also reads:

$$\delta^2 E_c(t) = \int_{\Gamma_o} \delta F_i \delta u_i dS_o + \int_{V_o} \delta b_{o,i} \delta u_i dV_o - W_2 \quad (4)$$

In addition, by considering the two-order Taylor expansion of kinetic energy, it can shown that:

$$\delta^2 E_c(t) = 2(E_c(t + \delta t) - E_c(t)) \quad (5)$$

In combination with Eq. (4), starting from an equilibrium configuration at time t ($E_c(t) = 0$), and thereafter ignoring changes in body forces, it follows that:

$$2E_c(t + \delta t) = \int_{\Gamma_o} \delta F_i \delta u_i dS_o - W_2 \quad (6)$$

Equation (6) is the fundamental equation that relates the kinetic energy of the system to the second-order work: the kinetic energy, immediately after an equilibrium state and in absence of change in body forces, appears as the difference between a boundary term, $B_2 = \int_{\Gamma_o} \delta F_i \delta u_i dS_o$, involving the loading path applied to the boundary of the system, and a volume term, $W_2 = \int_{V_o} \delta \Pi_{ij} \frac{\partial(\delta u_i)}{\partial X_j} dV_o$, which is related to the constitutive behaviour of the material. Equation (6) shows that necessarily $B_2 - W_2 \geq 0$, the equality being obtained for a quasi-static incremental evolution between two equilibrium states.

According to Eq. (6), the existence of an outburst in kinetic energy ($E_c(t + \delta t) > 0$) is related to a conflict between the loading prescribed to the boundary of the system and the

mechanical response of the system directed by its constitutive behavior. An interesting situation corresponds to the case where integral B_2 is nil. In that case, the existence of an outburst in kinetic energy is directly related to the vanishing of the second-order work. The loading applied to the system is assigned to remain constant ($B_2 = 0$), and the specimen fails (the kinetic energy rises abruptly) under the application of a certain class of disturbance for which the second-order work takes negative values. The equilibrium configuration is no longer sustainable [12,10].

2.2 Loss of sustainability of a cubic specimen

Hereafter, for convenience purposes, terms ε_{ii} and σ_{ii} are denoted ε_i and σ_i , respectively. If the specimen considered is a cube, in which the stress-strain state is reputed to be homogeneous, then Eq. (6) reads:

$$2E_c(t + \delta t) = V \delta s_i \delta \varepsilon_i - W_2 \quad (7)$$

where s_i denotes the external normal stress applied to the side 'i' of normal \underline{x}_i . The external stress components s_i should not be confused with the principal stress components σ_i acting on the internal face of side 'i' of the specimen. Equality between the two is obtained in any equilibrium configuration, and the equality between the incremental components δs_i and $\delta \sigma_i$ is achieved along any quasi-static transformation. In this case, incremental stress components δs_i and $\delta \sigma_i$ relate to the incremental strain $\delta \varepsilon_i$ as follows:

$$\delta s_i = \delta \sigma_i = K_{ij} \delta \varepsilon_j \quad (8)$$

where \underline{K} is the tangent constitutive operator written here in the coinciding principal stress-strain axes. If the loading is kinematically prescribed, terms $\delta \varepsilon_j$ act as control parameters, and terms δs_i stand as response parameters. More generally, the loading can be described by a mixed control vector \underline{C} , whose components are composed of linear combinations of stress components and of linear combinations of strain components.

Thus, vector \underline{C} can be expressed as:

$$C_i = A_{ij} s_j, \text{ for } i = 1, \dots, p \quad (\text{static control parameters}) \quad (9)$$

$$C_i = B_{ij} \varepsilon_j, \text{ for } i = p + 1, \dots, 3 \quad (\text{kinematic control parameters}) \quad (10)$$

where \underline{A} and \underline{B} are two matrices, respectively, of dimension $(p \times 3)$ and $((3 - p) \times 3)$. The three components C_i are referred to as the control parameters. To be more specific, $p = 1$ in the following (note that $p = 2$ can be treated in the same way).

Without altering the generality of the problem, the response vector \underline{R} can be considered to be composed of stress or strain components:

$$R_1 = \varepsilon_1 \quad (11)$$

$$R_i = s_i, \text{ for } i = 2, 3 \quad (12)$$

Moreover, as both control and response parameters must be conjugated with respect to energy, the following relations hold in the large and in the small:

$$C_i R_i = s_i \varepsilon_i \quad \text{and} \quad \delta C_i \delta R_i = \delta s_i \delta \varepsilon_i \quad (13)$$

Taking constitutive relation (8) into account, the second-order work can be written as:

$$W_2 = V \delta \sigma_i \delta \varepsilon_i = V K_{ij} \delta \varepsilon_i \delta \varepsilon_j = V K_{ij}^s \delta \varepsilon_i \delta \varepsilon_j \quad (14)$$

Combining Eq. (7) with Eqs. (13) and (14) yields:

$$2E_c(t + \delta t) = V \delta C_i \delta R_i - V K_{ij}^s \delta \varepsilon_i \delta \varepsilon_j \quad (15)$$

By definition, the mechanical state considered belongs to the bifurcation domain if \underline{K}^s admits at least one negative eigenvalue. In that case, directions \underline{x} exist such that $K_{ij}^s x_i x_j < 0$. In the three-dimensional space, such a direction corresponds to the intersection of two planes, of equations $\alpha_i x_i = 0$ and $\beta_i x_i = 0$. Now, let B_{2i} and B_{3i} be equal to α_i and β_i , respectively. Thus, $C_2 = \alpha_i \varepsilon_i$ and $C_3 = \beta_i \varepsilon_i$.

If both control parameters C_2 and C_3 are assigned to remain constant, $\alpha_i \delta \varepsilon_i = 0$ and $\beta_i \delta \varepsilon_i = 0$. Therefore, the vector $\delta \underline{\varepsilon}$ is such that $K_{ij}^s \delta \varepsilon_i \delta \varepsilon_j < 0$. The vector $\delta \underline{\varepsilon}$ is associated with a negative value of the second-order work. Moreover, if C_1 is also assigned to remain constant (usually at an extremum), Eq. (15) takes the following straightforward form:

$$2E_c(t + \delta t) = -V K_{ij}^s \delta \varepsilon_i \delta \varepsilon_j \quad (16)$$

Equation (16) indicates that the incremental evolution of the system from the equilibrium configuration considered, and under the loading prescribed by a constant value of the parameters C_1 , C_2 and C_3 , is associated with a strictly positive value of the kinetic energy. Thus, if a (certain) disturbance is applied to the specimen, the evolution of the system, characterised by an incremental strain $\delta \underline{\varepsilon}$, will induce an increase in the kinetic energy according to Eq. (16). There is a transition from a quasi-static regime toward a dynamic regime, under continuous change in the loading parameters (indeed constant). This is therefore a proper bifurcation phenomenon.

These theoretical results are carefully checked using a discrete numerical model in the following sections.

3 A discrete element method model

3.1 YADE software

Numerical investigations based on the discrete element method [4] were conducted with the open-source software

YADE [8]. The discrete element method models granular materials as collections of rigid locally deformable bodies. The interactions between particles are described by inter-particle interaction laws. The interaction law used in this paper involved three constant mechanical parameters k_n , k_t and φ_g . k_n is the elastic stiffness contact in the normal direction to the tangent contact plane (no tensile normal force is allowed). In the tangential direction, the elastic stiffness contact is represented by k_t and the tangential contact force obeys the Coulomb friction law characterised by the friction angle φ_g .

The numerical model consists of an assembly of spherical particles forming a cubical specimen. The particle assembly is enclosed within six rigid and frictionless walls. The external stress–strain state is imposed on the specimen by acting on wall positions, either directly for a strain control or indirectly through a closed-loop control for a stress control. Strain and stress responses are computed at the boundary of the specimen, from the wall displacements for strains and from particle-wall contact forces for stresses.

3.2 Numerical specimens

Numerical simulations were conducted with specimens made up of 150,000 spherical grains, whose diameter ranges from 2 to 12 mm. The normal stiffness k_n at the contact between two granules is equal to $356 \cdot D_s$ (MPa), where D_s is the mean diameter of the two granules. The tangent stiffness k_t at the contact between granules is equal to $0.42 \cdot k_n$. The friction angle φ_g is fixed at 35° . A loose specimen was considered with an initial porosity equal to 0.41. The granular assembly was first subjected to an isotropic compression, at different confining pressures σ_3 (50, 100 and 150 kPa). Then, after each confining stage, a drained triaxial loading in axisymmetric conditions was simulated. The evolution of both the deviatoric stress $q = \sigma_1 - \sigma_3$ and the volumetric strain ε_v in terms of the axial strain ε_1 are given in Figs. 1 and 2. The deviatoric stress continuously increases (positive hardening regime) toward a limit plateau, and a contractant volumetric behavior is observed.

3.3 Existence of a bifurcation domain

Computation of the strain increment $d\varepsilon$ for each direction of the stress increment $d\sigma$ determines the normalised second-order work: $W_2 = \frac{d\sigma \cdot d\varepsilon}{\|d\sigma\| \|d\varepsilon\|}$. For convenience, a circular diagram is plotted [9], constituted by points of coordinates $(\cos \alpha_\sigma (0.5 + W_2), \sin \alpha_\sigma (0.5 + W_2))$, where $\tan \alpha_\sigma = \frac{\partial \sigma_1}{\sqrt{2} \partial \sigma_3}$. When the second-order work takes negative values, the diagram crosses the dashed circle of radius $r = 0.5$. Figure 3 shows circular second-order work diagrams, computed from the numerical specimen used in the previous

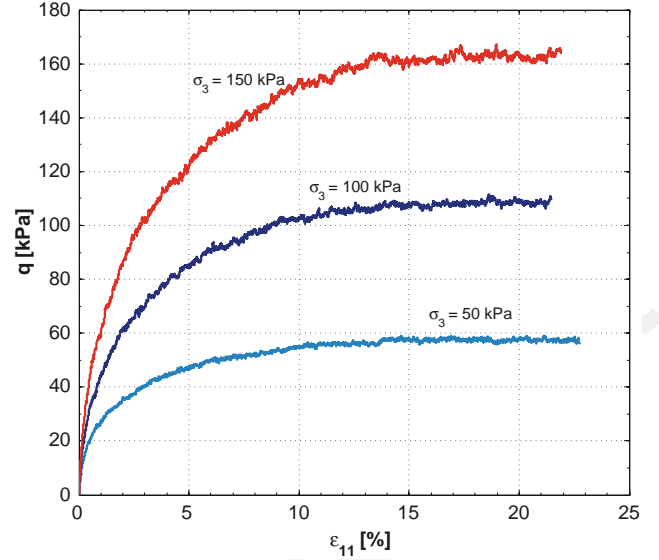


Fig. 1 Deviatoric stress over the axial strain at different confining pressures. Loose specimen

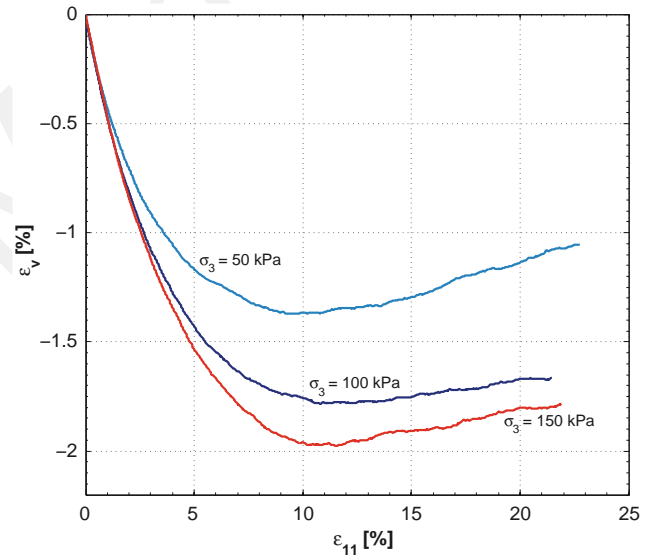


Fig. 2 Volumetric strain over the axial strain at different confining pressures. Loose specimen

section, at different deviatoric stresses under 100 kPa of confining pressure (points A, B and C in Fig. 1). It can be seen that the second-order work takes negative values along the stress direction contained within a cone, from a deviatoric stress q close to 60 kPa. The opening angle of the cone increases with the deviatoric stress ratio as the stress state approaches the Mohr-Coulomb failure line. These results show that the numerical sample possesses a wide bifurcation domain. The boundary of this domain, corresponding to the first vanishing of the second-order work (the first vanishing of $\det \underline{K}^s$), is clearly within the plastic limit surface, which means that

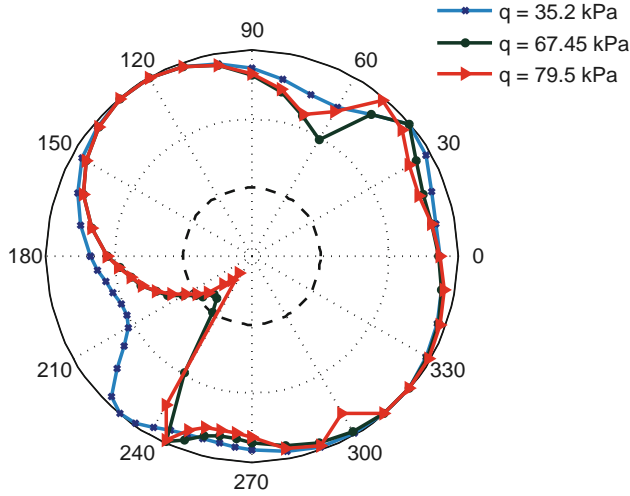


Fig. 3 Circular diagrams of the second-order work. Loose specimen under 100 kPa of confining pressure

many types of failure can be encountered well before the plastic limit is reached.

4 Simulation of the loss of sustainability

The simulations run in the previous section have shown that stress directions along which the second-order work takes negative values exist for the numerical specimen at a deviatoric stress $q = 79.5$ kPa. The corresponding mechanical state therefore belongs to the bifurcation domain. More specifically, the unstable cone (gathering all stress directions along which the second-order work takes negative values) is limited by two directions corresponding to $\alpha_\sigma = 215^\circ$ and $\alpha_\sigma = 235^\circ$. Adopting the notations introduced in Sect. 2, where both internal stress σ_i and external stress s_i are distinguished, the angle $\alpha_\sigma = 215$ is defined as $\tan \alpha_\sigma = \frac{ds_1}{\sqrt{2} ds_3}$. Setting $R = \frac{1}{\sqrt{2} \tan \alpha_\sigma}$, it follows that (in axisymmetric conditions):

$$ds_1 - \frac{1}{R} ds_3 = 0 \quad (17)$$

Let the (stress) control parameter $C_1 = s_1 - \frac{1}{R} s_3$ be introduced. Prescribing the control parameter C_1 to be constant ($dC_1 = 0$) corresponds to imposing a stress increment along the direction $\alpha_\sigma = \tan^{-1} \left(\frac{1}{\sqrt{2} R} \right)$. The second (strain) control parameter C_2 is defined so that Eq. (13) holds true. Thus, $C_2 = \varepsilon_1 + 2R \varepsilon_3$. Then, under a confining pressure $\sigma_3 = 100$ kPa and at a deviatoric ratio $\eta = 0.62$, both control parameters C_1 and C_2 are maintained constant. A very small disturbance is assigned to some grains belonging to the weak phase [14]. Typically, an impulse corresponding to a kinetic energy input of 5×10^{-6} J is applied to four grains chosen

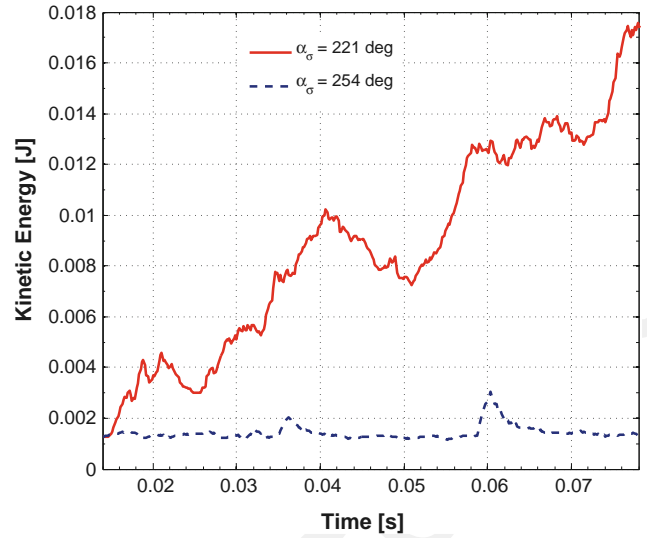


Fig. 4 Evolution over time of the kinetic energy within the specimen after a disturbance is applied

randomly within the weak phase. This kinetic energy input is very small with respect to the external work (on an order of magnitude of 10^{-1} J) provided to the specimen to reach the deviatoric stress ratio $\eta = 0.62$. Two different stress directions were investigated. The first direction, characterised by $\alpha_\sigma = 254^\circ$, was chosen outside the unstable cone. As observed in Fig. 4, the kinetic energy of the specimen (computed by summing the translational and the rotational kinetic energies of all the particles) does not increase significantly. The mechanical state of the specimen remains unchanged. Both stress and strain components do not vary over time after the application of the disturbance (not plotted here). On the contrary, a second stress direction characterised by $\alpha_\sigma = 221^\circ$ was chosen inside the unstable cone. The abrupt increase in kinetic energy after the application of the disturbance is clear (Fig. 4). In less than 0.1 s, the kinetic energy increases by 0.02 J, 4,000 times the kinetic energy provided to the specimen when applying the disturbance. The equilibrium state of the specimen cannot be sustained. The external stress loading can no longer be balanced by the internal stress whose components decrease. The specimen merely collapses.

These simulations corroborate the results obtained by Sibille very well, using different computational software [13–16]. These simulations, performed in different conditions, using different computational tools, reveal that granular materials may fail well before the standard Mohr-Coulomb failure limit is reached.

5 Concluding remarks

This paper has presented, within a unified framework, the notion of failure, described as the occurrence of an increase

in kinetic energy under constant loading parameters. Starting from an equilibrium state, a general equation was derived to express the increase in kinetic energy, as a function of both a boundary term involving the external loading and a constitutive term involving internal incremental strain and stress fields. It was shown that the boundary term, with a convenient choice of control parameters, could be assigned to be nil, whereas the constitutive term (also called second-order work) took a negative value. As a consequence, the kinetic energy starts to increase from an initial nil value (equilibrium state). These theoretical findings were perfectly ascertained from three-dimensional numerical simulations based on a discrete element method. In particular, it was thoroughly verified that three basic conditions must be fulfilled to give rise to a failure mechanism:

- The equilibrium state belongs to the bifurcation domain, in which the symmetric part of the tangent constitutive operator admits at least one negative eigenvalue. Indeed, the boundaries of the bifurcation domain are given by the surface where the determinant of that symmetric part of the constitutive operator vanishes first and by the plastic limit condition (vanishing of the constitutive determinant itself). In this domain, loading directions exist along which the second-order work takes negative values.
- The loading is controlled by mixed parameters, some being composed of stress components, the other of strain components.
- The mixed control parameters, when maintained constant, impose a loading direction associated with a negative value of the second-order work.

References

1. Bazant, Z., Cedolin, L.: *Stability of Structures*. Dover Edition Publ, USA (2003)
2. Challamel, N., Nicot, F., Lerbet, J., Darve, F.: On the stability of non-conservative elastic systems under mixed perturbations. *Eur. J. Env. Civil Eng.* **13**(3), 347–367 (2009)
3. Challamel, N., Nicot, F., Lerbet, J., Darve, F.: Stability of non-conservative elastic structures under additional kinematics constraints. *Eng. Struct.* **32**(10), 3086–3092 (2010)
4. Cundall, P.A., Strack, O.D.L.: A discrete numerical model for granular assemblies. *Geotechnique* **29**(1), 47–65 (1979)
5. Darve, F., Vardoulakis, I.: *Degradations and Instabilities in Geomaterials*. Springer, Berlin (2004)
6. Gudehus, G.: A comparison of some constitutive laws for soils under radially symmetric loading and unloading. In: Aachen, Witke, W. (eds.) *3rd International Conference on Numerical Methods in Geomechanics*, vol. 4, pp. 1309–1324. Balkema Publisher, (1979)
7. Hill, R.: A general theory of uniqueness and stability in elastic-plastic solids. *J. Mech. Phys. Solids* **6**, 236–249 (1958)
8. Kozicki, J., Donze, F.V.: A new open-source software developed for numerical simulations using discrete modeling methods. *Comp. Meth. Appl. Mech. Eng* **197**(49-50), 4429–4443 (2008)
9. Laouafa, F., Darve, F.: Modelling of slope failure by a material instability mechanism. *Comp. Geotech.* **29**(4), 301–325 (2002)
10. Nicot, F., Darve, F.: A micro-mechanical investigation of bifurcation in granular materials. *Int. J. Solids Struct.* **44**, 6630–6652 (2007)
11. Nicot, F., Challamel, N., Lerbet, J., Darve, F.: Mixed loading conditions, revisiting the question of stability in geomechanics. *Int. J. Num. Anal. Methods Geomech.* Article first published online: 2 SEP 2010. doi:10.1002/nag.959 (2010)
12. Nicot, F., Darve, F., Khoa, H.D.V.: Bifurcation and second-order work in geomaterials. *Int. J. Num. Anal. Methods Geomechanics* **31**, 1007–1032 (2007)
13. Nicot, F., Sibille, L., Darve, F.: Bifurcation in granular materials: an attempt at a unified framework. *Int. J. Solids Struct.* **46**, 3938–3947 (2009)
14. Radjai, F., Roux, S., Moreau, J.J.: Contact forces in a granular packing. *Chaos*, **9**, (n°3), 544–550 (1999)
15. Sibille, L., Donzé, F., Nicot, F., Chareyre, B., Darve, F.: Bifurcation detection and catastrophic failure. *Acta Geotechnica* **3**(1), 14–24 (2008)
16. Sibille, L., Nicot, F., Donzé, F., Darve, F.: Analysis of failure occurrence from direct simulations. *Eur. J. Environ. Civil Eng.* **13**(2), 187–202 (2009)
17. Thom, R.: *Stabilité Structurelle et Morphogénèse*. Interéditions Paris Publ, Paris (1972)
18. Vardoulakis, I., Goldscheider, M., Gudehus, G.: Formation of shear bands in sand bodies as a bifurcation problem. *Int. J. Numer. Anal. Meth. Geomech.* **2**(n°2), 99–128 (1978)
19. Vardoulakis, I.: Shear band inclination and shear modulus of sand in biaxial tests. *Int. J. Numer. Anal. Meth. Geomech.* **4**(2), 103–119 (1980)
20. Vardoulakis, I., Sulem, J.: *Bifurcation Analysis in Geomechanics*. Chapman & Hall Publisher, London (1995)
21. Wang, Y., Alonso-Marroquin, F.: A finite deformation method for discrete modeling, particle rotation and parameter calibration. *Granular Matter* **11**(5), 331–343 (2009)